Cloud phase identification over Arctic boundary layer clouds from airborne spectral cloud top reflectance measurements

André Ehrlich[1], Eike Bierwirth[1], Manfred Wendisch[1], Jean – Francois Gayet[2], Guillaume Mioche[2], Astrid Lampert[3]

[1] Institute for Atmospheric Physics, Johannes Gutenberg University, Mainz, Germany
[2] Laboratoire de Météorologie Physique (LAMP), Université Blaise Pascal, Aubière Cedex, France
[3] Alfred Wegener Institute for Polar and Marine Research, Potsdam, Germany

1. Introduction

Special Conditions in the Arctic

- Low sun elevation/high surface albedo → enhanced interaction of radiation with atmosphere
- Clouds (especially low-level) most important contributor to Arctic surface radiation budget
- Cloud forcing is highly variable and depends on:
  cloud water content, cloud particle size, **cloud thermodynamic phase**, surface albedo, aerosol

Cloud Thermodynamic Phase

- Increasing ice fraction (f_i=ice water content/total water content)
  → Increasing cloud top reflectance
  → Increasing cloud absorptance in near infrared wavelength range

→ Identification of cloud phase is a key point for remote sensing of cloud properties

2. SMART-Albedometer

(Spectral Modular Airborne Radiation measurements sysTem)

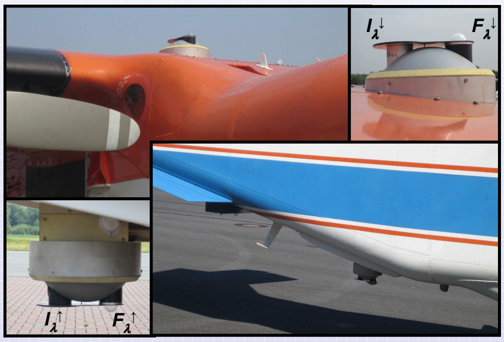

Fig. 1: The SMART-Albedometer mounted on the Polar 2 research aircraft. Close-ups show the optical inlets for irradiance F_λ (transparent semi-spheres) and radiance I_λ (flat opening). The grey cupola holding the inlets is automatically tilted for fast and accurate horizontal stabilization during flight.

Horizontal Stabilization of the Optical Inlets [1]

- Necessity for Arctic (θ_S = 70°)
  - $\Delta\theta$ = 0.2°→ ±2%
  - $\Delta\theta$ = 1.0°→ ±5% deviation in $F_\lambda\downarrow$
- Active system using servo motors
- Range ± 6°
- Accuracy of 0.2°
- Time response 43 ms for angular velocities up to 3° s^{-1}

Radiation Measurements

- 6 grating spectrometers
- 4 optical inlets for radiance I_λ and irradiance F_λ, connected to the spectrometers via fiber optics

	Measured Quantity	Spectral Range	Resolution
Airborne	Downwelling Irradiance $F_\lambda\downarrow$	310-1000 / 1000-2200 nm	2-3 / 9-16 nm
	Downwelling Radiance $I_\lambda\downarrow$	310-1000 nm	2-3 nm
	Upwelling Irradiance $F_\lambda\uparrow$	310-1000 nm	2-3 nm
	Upwelling Radiance $I_\lambda\uparrow$	310-1000 / 1000-2200 nm	2-3 / 9-16 nm

3. ASTAR 2007 (Arctic Study of Tropospheric Aerosol, Clouds and Radiation)

- Northern flow of cold air outbreak initiated convection over the warm ocean → low level clouds
- Ice, liquid water and mixed-phase clouds were observed
- Mixed-phase clouds showed liquid layer at cloud top precipitating ice below

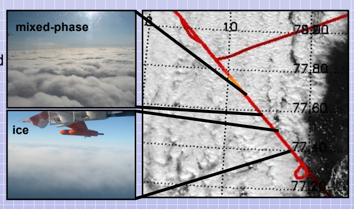

Fig. 2: Extract of the flight track of 7th April (first flight) along the CALIPSO track overlaid on the MODIS satellite image. On the cloud edge pure ice clouds were observed, while mixed-phase clouds dominated the interior of the cloud field.

Spectral Cloud Top Reflectance and Albedo

Reflectance $$R_\lambda = \pi I_\lambda^\uparrow / F_\lambda^\downarrow$$

Albedo $$\alpha_\lambda = F_\lambda^\uparrow / F_\lambda^\downarrow$$

- Dependent on: - Cloud optical depth τ
  - Cloud particle effective diameter D_{eff}
- Spectral pattern of ice and liquid water absorption in the wavelength range 1500 nm to 1800 nm

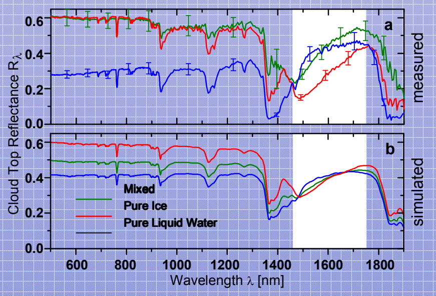

	water	mixed	ice
I_S	8.8	29.8	57.0
I_P	0.6	5.5	12.1
I_A	*	1.17	1.37

Fig. 3: Examples for cloud top reflectance. Measured reflectances (7th April) over a pure ice cloud (τ=12), pure liquid water cloud (τ=4) and mixed-phase cloud (τ=15) are given in panel a. Panel b shows simulations for pure ice, pure liquid water and mixed-phase clouds (τ=12).

4. Definition of Ice Indices

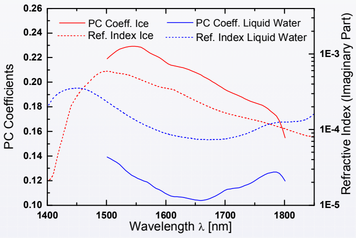

Fig. 4: Coefficients for the calculation of the principle components PC_I and PC_W (solid lines). Dashed lines represent the imaginary part of the refractive indices for ice and liquid water.

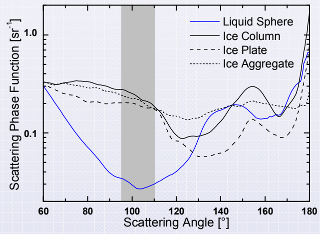

Fig. 5: Scattering phase function of different individual cloud particles at 640 nm wavelength. The diameter of the liquid water sphere is 16 µm. All ice crystals have maximum dimension of 55 µm.

Spectral Slope

- Using different absorption patterns of ice/liquid water
- Extended wavelength range to Acarreta et al. 2004 [2]

$$I_S = \frac{1}{R_{1640nm}} \left[\frac{dR}{d\lambda}\right]_{1550-1700nm}$$

Principle Component Analysis

- Using principle components PC_I and PC_W extracted from simulations of pure ice and liquid water clouds

$$I_P = \left(\frac{PC_I}{PC_W} - 0.57\right) \cdot 100$$

Reflectance - Albedo

- Arctic conditions with solar zenith angle ~70°
- Enhanced scattering into nadir direction of ice crystals (nonspherical) compared to liquid water particles (sphere) → higher anisotropy of radiation field
- Define anisotropy β_I and ice index I_A by

$$\beta_I = \frac{R_{645nm}}{\alpha_{645nm}} \qquad I_A = \frac{\beta_I^{meas}}{\beta_I^{water}\left(R_{645nm}^{meas}\right)}$$

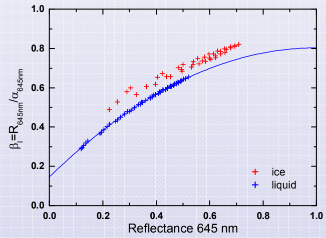

Fig. 6: Simulated β_I for pure liquid water clouds and pure ice clouds (column shaped crystals) of different optical thickness (τ=2-20) and effective diameter (9-26 µm for liquid water and 10-100 µm for ice clouds). Polynomial fits are overlaid as solid lines.

5. Case Study on April 7th

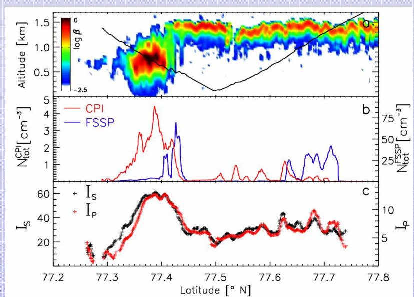

*Fig. 7: Profile of total attenuated backscatter coefficient **β** [sr^{-1} km^{-1}] for the cloud observed on April 7th (a). The flight altitude of the in situ measurements is overlaid as black line. Ice and liquid water particle concentration N_{tot} measured by CPI and FSSP along the flight track and the ice indices I_s and I_P for the same positions are given in panel b and c.*

Cloud Situation

- Low level mixed-phase cloud investigated
- CALIPSO lidar profile and in situ measurements show a detached ice cloud at the cloud edge 77.3° N to 77.4° N
- Precipitating ice, not capped by liquid water layer
- Liquid water 2 km from cloud edge
- High ice concentrations between 77.5° N to 77.6° N related to precipitating ice, low flight altitude

Ice Indices

- I_S and I_P along flight track identified ice cloud at the cloud edge I_S>40 I_P>10
- lower values from 77.45° N and further → mixed-phase cloud
- I_A of ice cloud highest β_I values
- I_A of mixed-phase clouds deviates from simulations for liquid water cloud → possible reasons
  - high measurement uncertainty
  - 3D radiative effects
  - ice crystals at cloud top

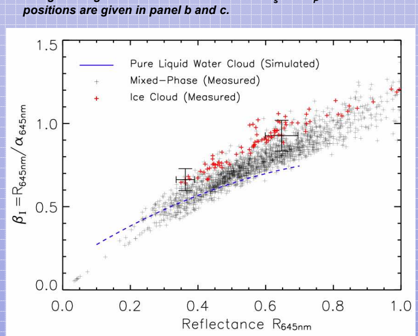

Fig. 8: Measured β_I as function of R_{645nm}. Black crosses show measurements over mixed-phase clouds; red crosses over the ice cloud observed on the cloud edge. Simulations for pure liquid water clouds are shown as blue line.

6. Outlook

- Investigation on horizontal distribution of ice/liquid water particles
- Aircraft measurement campaign SoRPIC (Solar Radiation and Phase Discrimination of Arctic Clouds) in September 2009 / between Svalbard and Scandinavia
  → Operating SMART-Albedometer on POLAR 5 (Alfred Wegener Institute for Polar Research)
  → Operating hyperspectral camera system Specim AISA Eagle
- Investigating 3D radiative effects based on measured horizontal distribution of ice and liquid water

[1] Wendisch, M., Muller, D., Schell, D., and Heintzenberg, J.: An airborne spectral albedometer with active horizontal stabilization, J. Atmos. Oceanic Technol., 18, 1856–1866, 2001.

[2] Acarreta, J. R., Stamnes, P., and Knap, W. H.: First retrieval of cloud phase from SCIAMACHY spectra around 1.6 µm, Atmos. Res., 72, 89-105, 2004.